ICAS 2016
30th Congress of the International Council of the Aeronautical Sciences
DCC, Daejeon, Korea ; September 25-30, 2016

EFFECT OF A 3D INDENTATION ON BOUNDARY LAYER INSTABILITY

Hui Xu*, Shahid Mughal*, Erwin R Gowree***, Spencer J Sherwin****
***Department of Mathematics, Imperial College London, UK**
****Department of Aeronautics, Imperial College London, London, UK**
*****Centre of Aeronautics, City University London, UK**
Keywords: *boundary layer, instability Navier-Stokes equations*

Abstract

We are concerned about effect of a 3D surface indentation on instability and laminar-turbulent transition in a boundary layer. For natural transition in a boundary layer, the transition onset is dominated by growth of the Tollmien-Schlichting (TS) wave and its subsequent secondary instability. In the paper, both linear analysis and nonlinear calculations are carried out to address the 3D surface indentation effect on amplifying TS waves' amplitudes and prompting transition onset. By the linear analysis, we address sudden amplification of the TS modes by a separation bubble in a surface indentation region. The nonlinear calculations are implemented to validate the traditional transition criteria predicted by the linear theory when a 3D indentation is present. Finally, applicability of the traditional transition criteria is assessed.

1 Introduction

Laminar-turbulent transition in boundary layers is a fundamental topic, understanding of which has special significances in science and engineering. However, transition process from laminar to turbulent flow poses a considerable theoretical and numerical challenge because of a strongly nonlinear process of transition. In a flat-plate boundary layer, laminar-turbulent transition can be triggered by growth of small-amplitude perturbation, such as Tollmiem-Schlichting (TS) waves. In environments with low levels of disturbances, transition to turbulence is initialised by the exponential amplification of TS waves and subsequent development of secondary instabilities. Breakdown to turbulence generally occurs when the amplitude of the primary instability typically research 10% of the free-stream velocity magnitude [1,2]. It is known that the linear stage can be described by the Orr-Sommerfeld (OS) equation and the traveling wave disturbances which evolve according to the OS equation are the so-called TS waves. Experimentally, the existence of TS waves was verified by Schubauer & Skramstad [3]. Mathematically, eigenvalues and eigenfunctions of the OS equation have been well described and studied [4,5,6]. Since the existence of TS waves was confirmed, there have been numerous studies undertaken to explore and explain transition. And various investigations have been implemented to understand mechanisms of TS waves' stabilisation and destabilisation. These mechanisms can be influenced by various factors, e.g. localised roughness elements. Recently, Xu *et al* [9] re-investigated the behaviour of TS waves undergoing small-scale localised distortions and found even a small separation bubble caused by a hump or an indentation can amplify a TS wave. Identifying the interaction between TS waves and a confined separation bubble can be important for natural transition. In 3D, Xu *et al* [10] did a further investigation.

For separation bubble on a flat-plate boundary layer, the separated shear layer can undergo rapid transition to turbulence and, even at rather small Reynolds numbers, separation provokes an increase in velocity perturbations and laminar breakdown, taking place in the separation region or close to it [7,8]. The concern in this paper is with evolution and amplification of planar 2D

TS waves in a boundary layer distorted by a 3D surface indentation where a thin separation

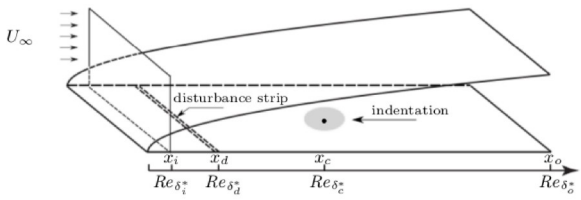

Fig.1 Schematic computational domain.

occurs. The schematic computational domain is shown in Fig. 1. The significance lies in addressing deformation of spanwise uniform 2D eigenmodes of a flat-plate boundary layer in a separation bubble, which will provide understanding of mechanism of transition onset. Moreover, assessment of the transition criteria is carried out when effect of a separation bubble comes into play and further, applicability of the transition criteria is assessed.

2 Formulations and Numerical strategy

2.1 The Navier-Stokes equations

Using the usual notations, the non-dimensional incompressible Navier-Stokes equations (NSEs) and continuity equation with constant density are given as follows

$$\partial_t u_i' - \nu_j^2 u_i' + u_j' \partial_j u_i' + \partial_i p' = 0 \quad (1)$$

$$\partial_j u_j' = 0, \text{in } \Omega' \quad (2)$$

A strategy to approach surface deformation is to employ a coordinate transformation which maps a deforming domain to a non-deforming one. Here, we consider a 3D time-independent surface deformation mapping from Ω' to Ω, which is defined by

$$x = x', \; y = y' - \zeta(x', z'), \; z = z' \quad (3)$$

where $\zeta(\cdot,\cdot)$ is the vertical displacement of the surface. Accordingly, the velocity components and pressure are transformed as follows

$$u = u', \; v = v' - u'\partial_{x'}\zeta - w'\partial_{z'}\zeta, \; w = w', p = p'. \quad (4)$$

Then, we can implement numerical calculations in a non-deforming domain.

The localised surface deformation $\zeta(\cdot,\cdot)$ is defined by

$$\zeta(x,z) = \begin{cases} -\frac{h}{2} \cdot \left(\cos\left(\frac{2\pi \cdot r}{\lambda}\right) + 1\right), & r \le \lambda/2, \\ 0, & r > \lambda/2, \end{cases} \quad (5)$$

where $r = \sqrt{(x' - x_c')^2 + (z' - z_c')^2}$ and λ is the maximum radial scale.

Generally, for an unstable frequency $\omega \in \mathbb{R}^+$, assuming the TS mode dependent on both x' and y', the TS wave envelope is defined by the absolute maximum amplitude of the TS wave as follows

$$A'(x', z') = \max\{|'(x', y', z', t)| : \forall y' \in [0, \infty), \forall\, t \in \mathbb{R}^+\}. \quad (6)$$

2.3 Numerical strategy

In order to get high precision and performance, a Fourier-spectral/hp element discretisation method, implemented in the Nektar++ package, is used in this work to solve the nonlinear as well as linearised Navier-Stokes equations. A stiffly stable splitting scheme is adopted which decouples the velocity and pressure fields and time integration is achieved by a second-order accurate implicit-explicit scheme [11,12].

For 2D calculations, with pre-desgined mesh, a convergence study by *p*-type refinement is performed to guarantee that mesh independence is achieved throughout this study. For 3D calculations, due to the non-deforming mapping, a spectral element discretisation can be used only in x-y plane, while a Fourier expansion is used in the spanwise z-direction. Along the spanwise direction, periodic boundary conditions are enforced. In order to implement linear analysis, for 3D base flow generation and fully nonlinear calculations, independence of spanwise Fourier modes is performed to guarantee that independence of both mesh and modes is achieved.

For base flow generation, in the whole computational domain, with respect to discrete temporal derivative, the L^2 relative error of velocity fields is less than 10^{-6}.

Once base flows are obtained, the linearised NSEs (LNSEs) is employed to address amplification of planar 2D TS waves and deformation of $A'(x', z')$ due to separation bubble confined with indentations.

3 Results

3.1 Flow configurations

Practically, the free-stream Reynolds number Re_f per meter is $1.2\text{x}10^6$/m. The reference free-stream velocity U_∞ equals 18m/s. Physical parameters are given in Table 1. The inlet position is located sufficiently far from the position of indentations, which guarantees that indentations' size has no influence on inlet velocity profile and allow base flows to recover the Blasius velocity profile. Physically, for all cases, the physical frequency is fixed and equals 172 (Hz) and the wavelength of the TS wave is equal to 34mm. Corresponding to the physical frequency, the non-dimensional frequency $F=2\pi f\nu/U_\infty^2 \times 10^6 = 50$. For all cases, indentations are located in the unstable regime of neutral stability curve as indicated in Fig. 2.

Group	Case	x_i(m)	x_c(m)	x_o(m)	f(Hz)	λ(mm)	h(mm)	L_x(m)	L_y(m)	L_z(m)
1	A	0.1	0.649	1.2	172	81	1.620	1.1	0.05	0.40
	B	—	—	—	—	—	1.895	—	—	—
	C	—	—	—	—	—	2.170	—	—	—
2	A	—	—	—	—	40.5	1.620	—	—	0.16
	B	—	—	—	—	—	1.895	—	—	—
	C	—	—	—	—	—	2.170	—	—	—

Table 1 Physical parameters

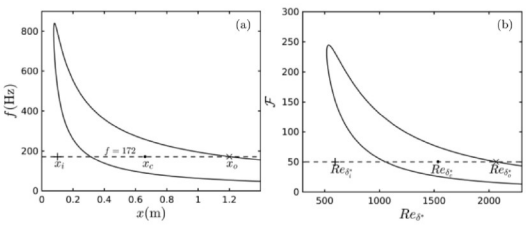

Fig.2 The reference neutral stability curve

3.2 Base flows

In Fig 3, we show the comparison between 2D base flows and 3D base flows in the plane z=0. We observe that the topological shapes of separation bubbles are different from each other. The 2D separation bubbles have the similar topological shapes but different size. Larger *h* gives rise to bigger bubble. For 3D cases, we see the bubble shapes are significantly different from each other in the planes z=0. We further observe that even for smallest depth *h*, the topological shape for the 2D separation bubble is different from the topological shape for the 3D separation bubble. For the largest depth *h*, the 2D separation bubble is completely confined within the indentation region and but the normal direction extension of the 3D separation bubble touches the surface y' = 0.

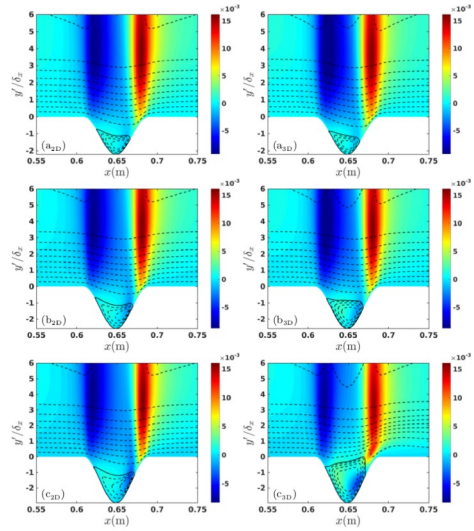

Fig 3. Comparison of 2D (Left) and 3D (Right) base flows. (Group 1)

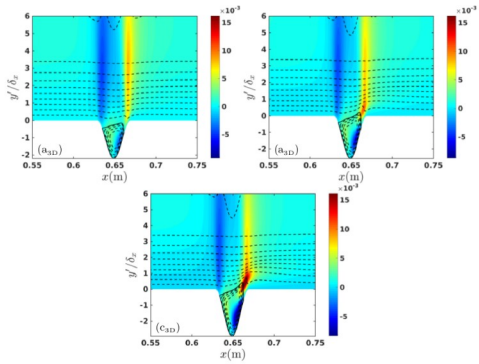

Fig 4. 3D base flows in planes z=0. (Group 2)

In Fig. 4, the base flows in the symmetric planes for the parameters from Group 2 are given. With the shortened width scale λ (=40.5 mm), we observe that in the planes z = 0, the separation bubbles occupy more area in the indentations, compared with the corresponding cases in Fig. 3. For the largest *h*, Fig 4(c_{3D}) shows that along the normal direction, the tip of the separation bubble protrudes from the indentation region and around the protruding tip, there exists a local region with a stronger vertical velocity

3.3 Properties of wall shear stress

Fig. 5(a_l-c_l) shows that for λ = 81(mm), the region coloured by red is clearly separated into two isolated subregions. Downstream of this region, a low shear region appears from the separation position. In figure 5(a_r -c_r), for λ = 40.5(mm), we observe that the separated

subregions of the region coloured in red occurs even for the smallest h. According to the separation bubbles in the plane z = 0 in Figs. 3 and 4, we deduce that the separated regions in the strong shear stress regions are attributed to the protrusions of the separation bubbles in the normal direction and the protruding tip separates the strong shear region into two sub region.

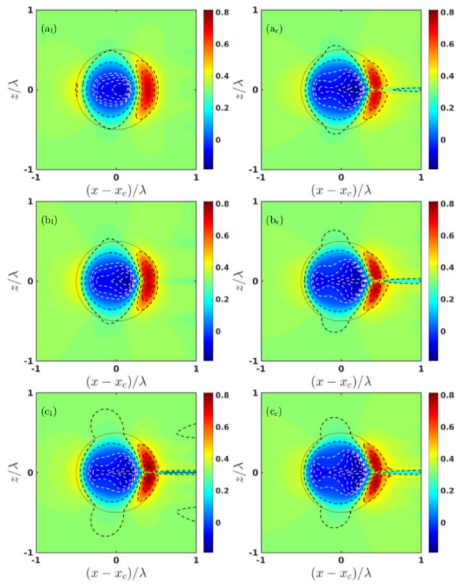

Fig.5 Comparison of $\partial u'/\partial\eta|_w$ on the wall: (Left) Group 1; (Right) Group 2.

3.4 Growth rate

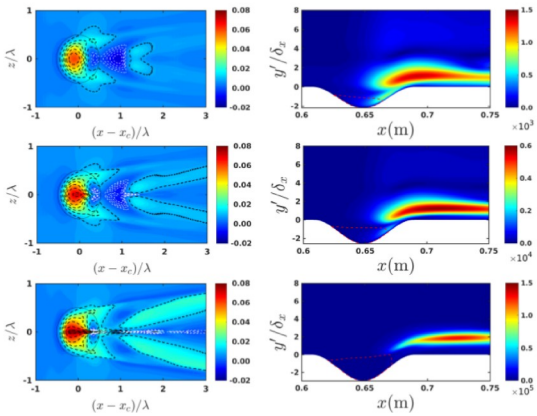

Fig. 6 Comparison of streamwise growth rate and TS amplitudes.

In Fig. 6, we observe that the TS modes growth contours for the parameters from Group 1 in Table 1 have significant changes and strong dependency on the parameters. In the regions of destabilising TS waves, the growth rates become greater and greater with the increasing parameter h. For Case A and Case B, there are two regions where the growth rates of TS waves decrease: one in the indentation region and another in the downstream region of the indention. The TS waves' stabilisation in these two regions are different from each other. The stabilisation region for Case A is connected, but for Case B, it is not a connected region and the downwstream stabilisation region has a thin wedge-like extension which splits the downstream destabilisation region into to separated regions. For Case C, the stabilisation regions are shrinking into very narrow regions which have longer distance downstream extensions. In the indentation regions, with the increasing h, destabilistion effects become stronger.

3.5 N-factors and transition

As we noted from Fig. 3, for smallest h (Case A), the 2D separation bubble is larger that the 3D separation bubble in the symmetric plane. This effect on N-factors show the magnitude of the 2D N-factor profile is greater than that of the 3D N-factor profile, which is clearly observed in the top sub-figure of Fig. 7. For Case B, when x < 0.8, the amplitude of the 2D N-factor profile is less than that of the 3D N-factor profile and when x > 0.8, the magnitude of the 2D N-factor profile is greater than that of the 3D N-factor profile. The downstream stabilisation region of the indentation elucidates the phenomenon, which is shown in Fig. 6. However, for the 3D case, N-factor is greater than 8 in the indentation region, which means strong nonlinear interaction, or even laminar-transition, can be triggered in the indentation region. For Case C, in the computational domain, the amplitude of the 3D N-factor profile is greater than that of the 2D N-factor profile and much greater than 8. A direct effect is that laminar-turbulent transition can occur suddenly in the 3D indentation region.

From the top subfigure of Fig. 8, we observe that laminar-turbulent transition onset is prompted because of base flow modulation and the onset occurs earlier than the prediction by the transition criteria. We derive that for the smallest h, the transition onset is dominated by nonlinear interaction between modulated base flow and TS modes, which accelerate the

breakdown of the spanwise flow structure. Therefore, the growth and the subsequent

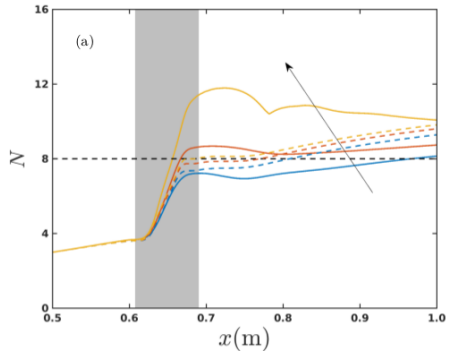

Fig. 7. Comparison of N-factors for 2D and 3D cases.

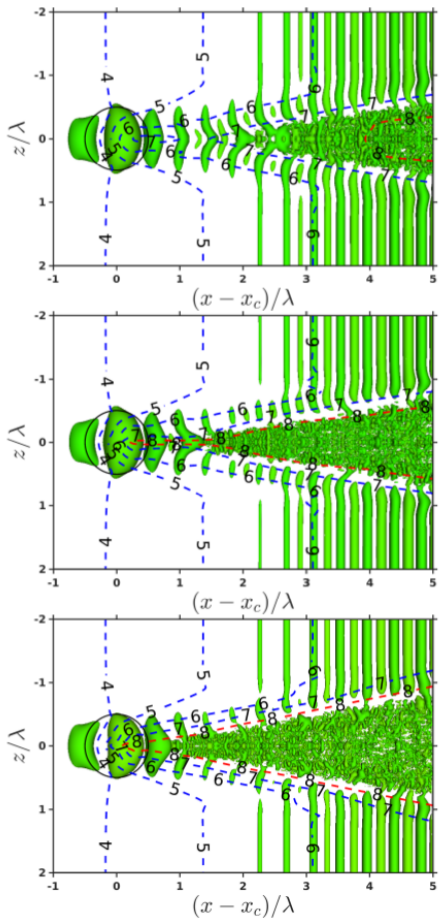

Fig. 8. Comparison of laminar turbulence transition onset

nonlinear effect of TS modes do not play the main role and the prediction of the transition onset by the N -factor criteria failed. Further, for Case B and Case C, we clearly observe that the N -factor values reach the transition criteria value 8 in the indentation regions. That is to say, strong nonlinear interaction, or even laminar-turbulent transition, occurs there. We realise that the transition onset and transition region predicted by the transition criteria N -factor are correct. We also notice that transition onset for Case C is earlier than that for Case B, although in the indentation regions, the transition criteria N -factor value is reached for the both cases. The phenomenon is attributed to that larger TS modes amplitudes give rise to stronger nonlinear interaction and quicker breakdown of the flows.

4. Conclusion

In this paper, we studied influence of a three dimensional indentation on the instability of a boundary layer. The study was done by linear analysis and nonlinear calculations. We only consider interaction of planar TS waves with two different types of 3D indentations. For each type, we fix the maximum radial length scale λ in x-z planes and change depth scale h. The scale λ for each case is comparable with the TS wavelength: (a) $\lambda/\lambda_{TS} = 2.38$; (b) $\lambda/\lambda_{TS} = 1.19$. For the parameters we investigated, there are separation bubbles in the indentation regions for both 2D and 3D cases.

As discussed in the paper, the variation of the depth *h*, topological shapes of 3D separation bubbles in the symmetric planes significantly changes compared with topological shapes of 2D separation bubbles. For 2D cases, the upper interfaces of the bubbles are concave, but for 3D cases, they are nearly flat. In the symmetrical planes, 3D separation bubbles intend to occupy more area in the indentation when depth h increases. Further, the 3D separation bubbles develop protrusions at the bubble tips which grow toward main stream. These differences are

attributed to 3D effect of the flows in the indentation regions, which result in that destabilisation impact of 3D separation bubbles in symmetric planes on the TS wave is significantly different from that of 2D separation bubbles. Further, we considered influence of varying maximum radial scale λ on base flows and planar TS waves. As observed from the figures, occurrences of separation bubble protrusions are common for 3D cases. In linear regime, from the contours of growth rate in x-z planes, we observed protrusions considerably amplify the TS wave.

Finally, we need to point out the transition prediction criteria, which is significantly influenced by indentation parameters, to some extent, can be used for deep indentation where the transition criteria N-factor value can be reached and strongly nonlinear interaction is dominated by growing TS modes. For shallow indentation, if the criteria N-factor value cannot be reached in the indentation region, the prediction strategy failed because 3D nonlinear interaction induced by indention modulation dominantly prompts transition onset. This provides a way to improve the transition prediction criteria.

Acknowledgements

This research was performed in the Laminar Flow Control Centre (LFC-UK) at Imperial College London. The Centre is supported by EPSRC under grant EP/I037946/1. The authors would also like to acknowledge support from Innovate UK and the United Kingdom Turbulence Consortium (UKTC) under grant EP/L000261/1 as well as from the Engineering and Physical Sciences Research Council (EPSRC) for access to ARCHER UK National Supercomputing Service (http://www.archer.ac.uk).

References

[1] Herbert T. Secondary instability of boundary-layers. Annu. Rev. Fluid Mech. Vol. 20, pp 487–526, 1988.

[2] Cossu C and Brandt L. Stabilization of Tollmien-Schlichting waves by finite amplitude optimal streaks in the blasius boundary layer. Phys. Fluids, Vol. 14, No. 8, pp L57–L60, 2002.

[3] Schubauer G B and Skramstad H K. Laminar-boundary-layer oscillations and transition on a flat plat. NASA TR-909, 1948.

[4] Stuart J T. Hydrodynamic stability. In Laminar Boundary Layer (ed. L. Rosenhead), pp. 492–579. Oxford University Press, 1963.

[5] Schlichting H. Boundary-Layer Theory, Mac Graw-Hill, 1968.

[6] Drazin P G and Reid W H. Hydrodynamic Stability, Combridge University Press, 1981.

[7] Browand F K. An experimental investigation of the instability of an incompressible separated shear layer, J. Fluid Mech., Vol. 26, No. 2, pp. 281–307, 1966.

[8] Rist U and Maucher U and Wagner S. Direct numerical simulation of some fundamental problems related to transition in laminar separation bubbles. In Computational Methods in Applied Sciences96 (ed. J. A. Desideri, C. Hirsch, P. Le Tallec, E. Onate, J. Periaux M. Pandolfi & E. Stein), pp. 319–325. John Wiley & Sons Ltd, 1996.

[9] Xu H, Sherwin S J, Hall P and Wu X S. The behaviour of Tollmien-Schlichting waves undergoing small-scale localised distortions, J. Fluid Mech., Vol. 792, pp 499–525, 2016.

[10] Xu H, Mughal S, Gowree E R and Sherwin S J. Influence of a three dimensional indentation on the instability of a boundary layer, preprint, 2016.

[11] Karniadakis G, Israeli M and Orszag S. High-order splitting methods for the incompressible navier-stokes equations, J. Comput. Phys., Vol. 97, No. 2, pp 414–443, 1991.

[12] Cantwell C D, Moxey D, Comerford A, Bolis A, Rocco G, Mengaldo G, Grazia D De, Yakovlev S, Lombard J E, Ekelschot D, Jordi B, Xu H, Mohamied Y, Eskilsson C, Nelson B, Vos P, Biotto C, Kirby R M and Sherwin S J, Nektar++: An open-source spectral/hp element framework. Computer Physics Communications, Vol. 192, pp 205–219, 2015.

Contact Author Email Address

hui.xu@imperial.ac.uk

Copyright Statement

The authors confirm that they, and/or their company or organization, hold copyright on all of the original material included in this paper. The authors also confirm that they have obtained permission, from the copyright holder of any third party material included in this paper, to publish it as part of their paper. The authors confirm that they give permission, or have obtained permission from the copyright holder of this paper, for the publication and distribution of this paper as part of the ICAS proceedings or as individual off-prints from the proceedings.